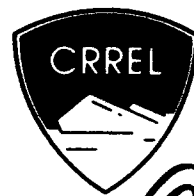


AD-A275 215



DTIC  
ELECTE  
JAN 3 1994  
S B D



2

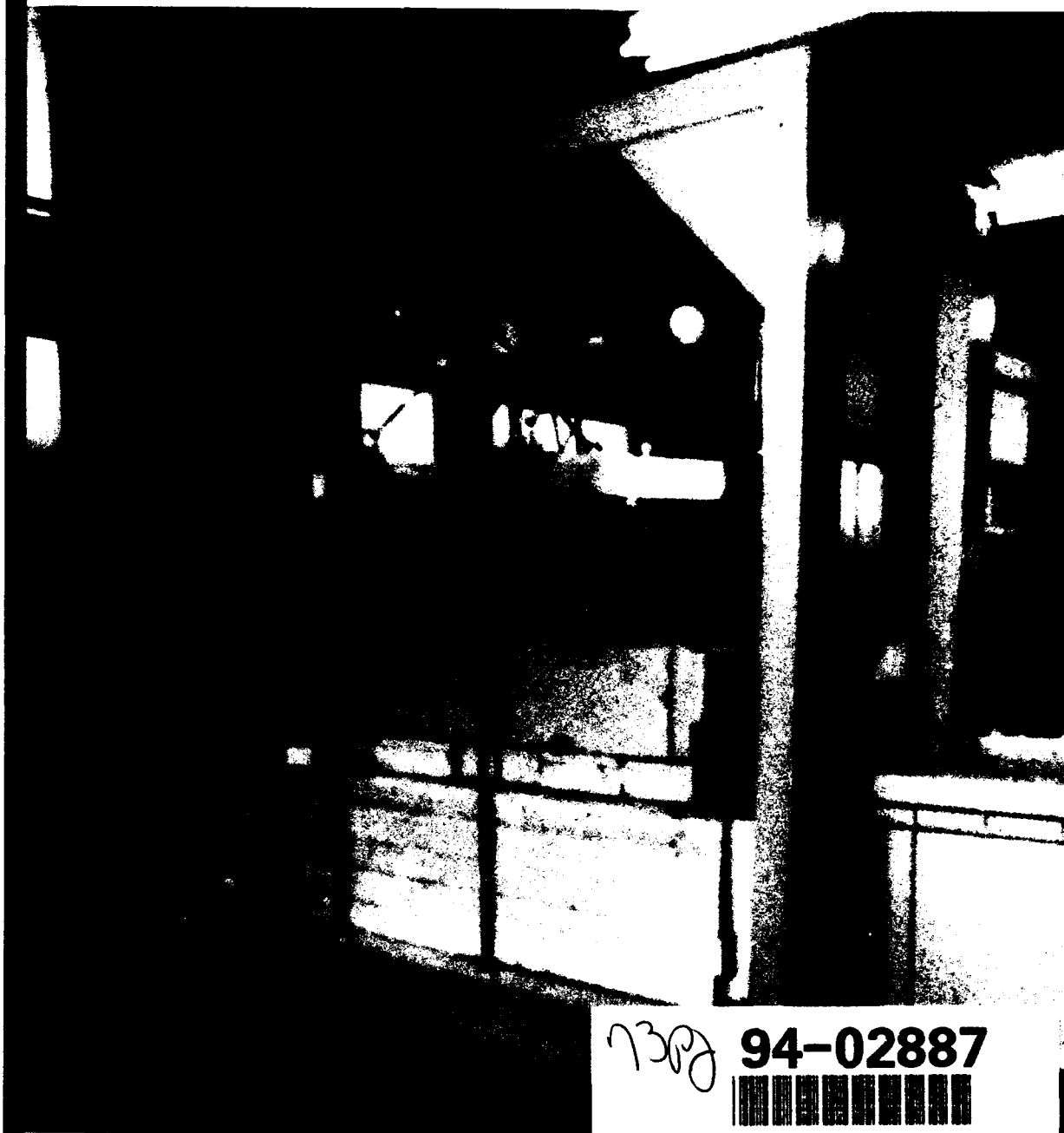
**DISTRIBUTION STATEMENT A**

Approved for public release  
Distribution Unlimited

# Growth Condition of an Ice Layer in Freezing Soils Under Applied Loads I. Experiment

Kazuo Takeda and Yoshisuke Nakano

November 1993



7302

94-02887



### ***Abstract***

A series of freezing tests on Kanto loam were conducted under various overburden pressures to find the steady growth condition of a segregated ice layer. The steady growth condition was found to be determined by the absolute value of the temperature gradient of the unfrozen part of the soil  $\alpha_u$  near the 0°C isotherm and that of the frozen part of the soil  $\alpha_f$  near the warmest end of an ice layer under given hydraulic conditions and applied effective pressure  $\sigma$  as follows:  $\alpha_u = A\alpha_f k_f/k_0 > A > S(\sigma)$ ; where  $k_f$  and  $k_0$  are the thermal conductivities of the frozen and unfrozen parts, respectively,  $A$  is a constant and  $S$  is an increasing function of  $\sigma$ . This is the first of a two-part presentation on the subject; the analytical aspects of the study are presented in a second report.

*Cover: Apparatus for testing ice growth in soils under applied loads. (Photo by K. Takeda.)*

For conversion of SI metric units to U.S./British customary units of measurement consult *Standard Practice for Use of the International System of Units (SI)*, ASTM Standard E380-89a, published by the American Society for Testing and Materials, 1916 Race St., Philadelphia, Pa. 19103.



**US Army Corps  
of Engineers**

**Cold Regions Research &  
Engineering Laboratory**

## **Growth Condition of an Ice Layer in Freezing Soils Under Applied Loads**

### **I. Experiment**

Kazuo Takeda and Yoshisuke Nakano

November 1993

Prepared for  
OFFICE OF THE CHIEF OF ENGINEERS

Approved for public release; distribution is unlimited.

## PREFACE

This report was prepared by Dr. Kazuo Takeda of the Technical Research Institute, Konoike Construction Co., Ltd., Konohana, Osaka, Japan, and Dr. Yoshisuke Nakano, Chemical Engineer, Applied Research Branch, Experimental Engineering Division, U. S. Army Cold Regions Research and Engineering Laboratory. Funding for this research was provided by DA Project 4A161102AT24, *Research in Snow, Ice and Frozen Ground*, Task SC, Work Unit F01, *Physical Processes in Frozen Soil*.

The authors thank Dr. V.J. Lunardini and Dr. Y.C. Yen of CRREL for technical review of this report.

The contents of this report are not to be used for advertising or promotional purposes. Citation of brand names does not constitute an official endorsement or approval of the use of such commercial products.

## CONTENTS

Preface .....	ii
Nomenclature .....	iv
Introduction .....	1
Experiment .....	3
Test results .....	6
Conclusions .....	12
Literature cited .....	11
Abstract .....	13

## ILLUSTRATIONS

### Figure

1. A steadily growing ice layer in a freezing soil .....	1
2. Temperature gradients $\alpha_1$ and $\alpha_0$ .....	2
3. Test apparatus and test cell .....	4
4. Consolidation characteristics of Kanto loam .....	5
5. Measured variables vs. time for $\sigma = 195$ kPa .....	6
6. Steady growth region $R_2$ .....	9
7. Values of $S(\sigma)$ vs. $\sigma$ .....	10

## TABLES

### Table

1. Test conditions .....	6
2. Summary of test results .....	8

**DRG QUALITY IMPROVEMENT**

<b>Accession For</b>	
NTIS GRA&I	<input checked="" type="checkbox"/>
DTIC TAB	<input type="checkbox"/>
Unannounced	<input type="checkbox"/>
Justification	
By	
Distribution/	
Availability Codes	
Dist	Avail and/or Special
A-1	

## NOMENCLATURE

$a_i$	constant defined by eq 3 where $i = 0, 1$
$A$	constant
$A_i$	constant where $i = 0, 1$
$d_i$	density of the $i$ th constituent
$e$	void ratio
$f_i$	mass flux of the $i$ th constituent relative to that of soil minerals where $i = 1, 2$
$f_{10}$	mass flux of water in the unfrozen part of the soil
$h$	amount of heave
$k_0$	thermal conductivity of the unfrozen part of the soil
$k_1$	thermal conductivity of an ice layer
$K_i$	empirical function defined by eq 8a where $i = 1, 2$
$K_{i1}$	limiting value of $K_i$ as $x$ approaches $n_1$ while $x$ is in $R_1$ , $i = 1, 2$
$L$	latent heat of fusion of water, $334 \text{ J g}^{-1}$
$m$	location of the top end of the specimen
$M_i$	name of a model where $i = 1, 2, 3$
$n$	boundary in $R_0$ where the pressure of water is specified
$n_i$	boundary with $i = 0, 1$ where $n_0$ denotes the boundary where $T = 0^\circ\text{C}$ and $n_1$ the interface between an ice layer and a frozen fringe
$P_i$	pressure of the $i$ th constituent where $i = 1, 2$
$P_{10}$	value of $P_1$ at $n_0$
$P_{21}$	value of $P_2$ at $n_1$
$r$	rate of frost heave
$R_0$	unfrozen part of the soil
$R_1$	frozen fringe
$R_2$	ice layer
$R_m$	region in the diagram of temperature gradients where an ice layer melts
$R_s$	region in the diagram of temperature gradients where the steady growth of an ice layer occurs
$R_s^*$	boundary between $R_s$ and $R_u$
$R_s^{**}$	boundary between $R_m$ and $R_s$
$R_u$	region in the diagram of temperature gradients where the steady growth of an ice layer does not occur
$S$	defined by eq 10
$S_0$	value of $S$ when $\sigma = 0$

$SP_o$	defined by eq 2
$t$	time
$T$	temperature
$T_1$	temperature at $n_1$
$T_1^{**}$	temperature at $n_1$ when eq 1 holds true
$T_c$	temperature of the cold bath
$T_w$	temperature of the warm bath
$x$	spatial coordinate
$\alpha_o$	absolute value of the temperature gradient at $n_o$
$\alpha_1$	absolute value of the limiting temperature gradient as $x$ approaches $n_1$ while $x$ is in $R_2$ , defined by eq 5
$\alpha_f$	absolute value of the temperature gradient near $n_1$ in $R_2$
$\alpha_u$	absolute value of the temperature gradient near $n_o$ in $R_o$
$\gamma$	constant, $1.12 \text{ MPa } ^\circ\text{C}^{-1}$
$\sigma$	effective pressure defined by eq 1
$i$	subscript denotes the $i$ th constituent of the mixture consisting of unfrozen water ( $i = 1$ ), ice ( $i = 2$ ) and soil minerals ( $i = 3$ )
*	superscript used to indicate the value of any variable evaluated when a point ( $\alpha_1, \alpha_o$ ) in the diagram of temperature gradients is on $R_s^*$
**	superscript used to indicate the value of any variable evaluated when a point ( $\alpha_1, \alpha_o$ ) in the diagram of temperature gradients is on $R_s^{**}$

# Growth Condition of an Ice Layer in Freezing Soils Under Applied Loads

## I. Experiment

KAZUO TAKEDA AND YOSHISUKE NAKANO

### INTRODUCTION

When moist fine-grained soil freezes, it often is accompanied by volume expansion caused by the appearance of layers of more or less pure segregated ice within the soil. The scientific investigation of segregated ice began in the early 1900s, but the understanding gained by Taber (1929, 1930), Beskow (1935) and others, although useful, was largely qualitative. Since then a significant amount of effort has been made to gain a quantitative understanding on ice segregation.

We will consider the one-directional steady growth of an ice layer. Let the freezing process advance from the top down and the coordinate  $x$  be positive upwards with its origin fixed at some point in the unfrozen part of the soil. A transitional zone, often referred to as the frozen fringe, exists between the frost front ( $0^\circ\text{C}$  isotherm) and the growing surface of an ice layer, though the nature of this zone has not been well understood. A freezing soil in this problem may be considered to consist of three parts: the unfrozen part  $R_0$ , the frozen fringe  $R_1$  and the ice layer  $R_2$ , as shown in Figure 1.

Radd and Oertle (1973) studied the relationship between the pressure  $P_{21}$  and the temperature  $T_1$  of an ice layer at  $n_1$  by using a water-permeable, constant-volume cell in which the unfrozen part of a soil column was connected with a water reservoir subjected to an atmospheric pressure,  $P_1 = 0.1$  (MPa). They found that there is a unique temperature  $T_1^{**}$  for given  $P_{21}$  and  $P_1$  when an existing ice layer neither grows nor melts and the flux of water  $f_1$  vanishes, and that  $T_1^{**}$  is given as:

$$\sigma = P_{21} - P_1 = -\gamma T_1^{**}, \quad \text{if } f_1 = 0 \quad (1)$$

where  $\sigma$  and  $P_{21}$  are often referred to as the effective pressure and the overburden pressure, respectively, and  $\gamma$  is a constant with the value of  $1.12 \text{ MPa } ^\circ\text{C}^{-1}$ . Equation 1 is often called the generalized Clausius-Clapeyron equation, which is attributed to Edlefsen and Anderson (1943). Studying the relationship between the effective pressure  $\sigma$  and  $T_1^{**}$  by using a closed constant-volume cell, Takashi et al. (1981) confirmed the validity of eq 1.

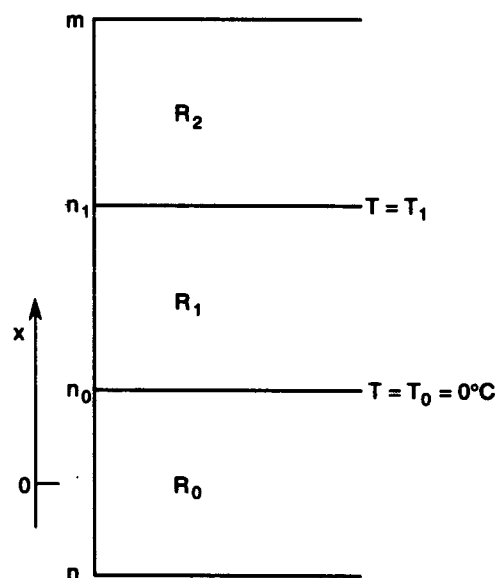


Figure 1. A steadily growing ice layer in a freezing soil.



Konrad and Morgenstern (1980, 1981, 1982) empirically found that the rate of water intake,  $f_{10}$ , at the formation of the final ice lens is proportional to the average temperature gradient  $(T')_a$  in the frozen fringe when a soil sample freezes under different cold-side step temperatures but the same warm-side temperature under atmospheric conditions. This may be written as:

$$f_{10} = -SP_0(T')_a \quad (2)$$

where a prime denotes differentiation with respect to  $x$ . The positive proportionality factor  $SP_0$  was found to be constant for a given soil and was termed the segregation potential. They also found empirically that  $SP_0$  depends on the pressure of water  $P_{10}$  at  $n_0$  and the applied pressure  $\sigma$ .

Studying the relationship between  $f_{10}$  and  $(T')_a$  experimentally, Ishizaki and Nishio (1985) confirmed the validity of eq 2 at the formation of the final ice lens. They also found that  $f_{10}$  is a linear function of the temperature difference,  $\Delta T = T_1^{**} - T_1$ , during the stable growth period of the final ice lens, namely:

$$\Delta T = a_0 + a_1 f_{10} \quad (3)$$

$$\Delta T = T_1^{**} - T_1 \quad (4)$$

where  $a_0$  and  $a_1$  are constants. Nakano and Takeda (1991) confirmed empirically the validity of eq 3 when  $\sigma = 0$ .

We studied mathematically and experimentally the steady growth condition of an ice layer under negligible applied pressure in three earlier reports in this series (Nakano 1990, Takeda and Nakano 1990, Nakano and Takeda 1991). We have shown that for a given hydraulic condition the steady growth condition is determined by the absolute value of the temperature gradient  $\alpha_0$  at  $n_0$  and the limiting value of the temperature gradient  $\alpha_1$  in  $R_2$  defined as:

$$\alpha_1 = - \lim_{\substack{x \rightarrow n_1 \\ x \text{ in } R_2}} T'(x). \quad (5)$$

The steady growth condition is presented in the diagram of temperature gradients as shown in Figure 2. The steady growth occurs in the region  $R_s$  bounded by  $R_s^{**}$  and  $R_s^*$ . The boundary  $R_s^{**}$  is a straight line given as

$$\alpha_0 = (k_1/k_0) \alpha_1 \quad (6)$$

where  $k_1$  and  $k_0$  are the thermal conductivities of  $R_2$  and  $R_0$ , respectively. We will refer to the region as  $R_m$  where  $\alpha_0 > (k_1/k_0)\alpha_1$ ,  $f_{10} < 0$  and an ice layer is melting. It should be mentioned that an existing ice layer neither grows nor melts,  $f_{10}$  vanishes and eq 1 holds true on  $R_s^{**}$ .

The boundary  $R_s^*$  is approximately a straight line given as:

$$\alpha_0 = S_0 \alpha_1 \quad k_1 k_0^{-1} > S_0 > 0 \quad (7)$$

where  $S_0$  is a constant that depends on only the properties of a given soil if  $\alpha_0 > 2.0$  ( $^{\circ}\text{C cm}^{-1}$ ). The steady growth of an ice layer does not occur in the region  $R_u$  where  $\alpha_0 < S_0 \alpha_1$ .

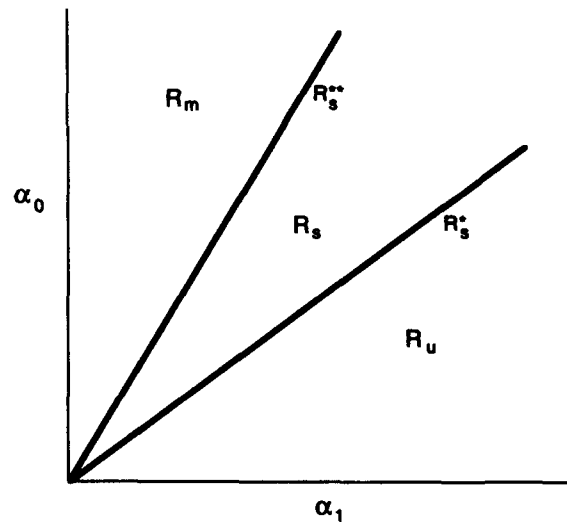


Figure 2. Temperature gradients  $\alpha_1$  and  $\alpha_0$ .

We introduced a model  $M_1$  (Nakano 1990) of a frozen fringe where ice may exist but does not grow, and the mass flux of water  $f_1 (= f_{10})$  is given as

$$f_1 = -K_1 \frac{\partial P_1}{\partial x} - K_2 \frac{\partial T}{\partial x} \quad \text{for } x \text{ in } R_1 \quad (8a)$$

$$K_2/K_1 \rightarrow \gamma \quad \text{as } f_1 \rightarrow 0 \quad (8b)$$

$$\lim_{\substack{x \rightarrow n_1 \\ x \text{ in } R_1}} P_1(x) = P_2(n_1) = P_{21} \quad (8c)$$

where  $K_1$  and  $K_2$  are properties of a given soil that generally depend on  $T$  and the composition of the soil.

In the three earlier reports in this series we showed that  $M_1$  is consistent with eq 1 (Nakano 1990), eq 3 and 7 under  $\sigma = 0$  (Nakano and Takeda 1991). We also showed (Nakano and Takeda 1991) that the boundary  $R_s^*$  under  $\sigma = 0$  is given as:

$$\alpha_0 = k_1 (k_0 + LbK_{21}^*)^{-1} \alpha_1 \quad (9)$$

where  $L$  is the latent heat of fusion of water,  $b$  is a function of the thickness  $\delta$  of  $R_1$  defined by eq 73c and 73e in Nakano (1990), and  $K_{21}$  is the limiting value of  $K_2$  as  $x$  approaches  $n_1$  while  $x$  is in  $R_1$ . An asterisk denotes that  $K_{21}^*$  is the value of  $K_{21}$  when a point  $(\alpha_1, \alpha_0)$  is on  $R_s^*$  in the diagram of temperature gradients.

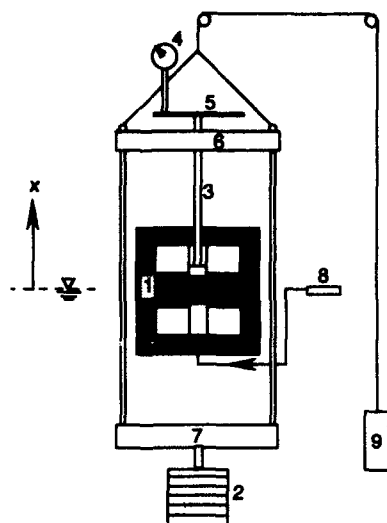
This is the first of a two-part presentation on the effects of applied pressure on the steady growth condition of an ice layer. The objective of this work is to show empirically how the applied pressure affects the steady growth condition of an ice layer. In the following work we will show that the model  $M_1$  is consistent with experimental data presented in this work. Moreover, we will show that  $M_1$  is consistent with the reported empirical relationships, such as eq 2 and 3, under applied pressure.

## EXPERIMENT

The same test apparatus used in the previous study (Takeda and Nakano 1990) was combined with a loading device that imposed a specified effective pressure  $\sigma$  on a test specimen as shown in Figure 3a. Since the weight of this loading device is balanced by the counterweight, only a specified and constant pressure  $\sigma$  is applied on the moving top surface of the specimen, provided that the friction of the suspending wire for the counterweight is negligibly small. However, the friction of the wire is not negligible when  $\sigma$  is small. Therefore, a weight was applied directly on the top of the specimen when  $\sigma$  was less than 50 kPa. Figure 3b is a photograph of the test apparatus.

A schematic drawing of the test cell is shown in Figure 3c. The test cell used in this study is essentially the same as that used in Takeda and Nakano (1990) except for minor modifications described below. In order to improve the accuracy of temperature measurements, one more thermocouple was added at  $x = -1.0$  cm in the center of the unfrozen part of the specimen where a one-dimensional coordinate  $x$  is introduced with its origin at the level of the water reservoir, as shown in Figure 3a. Hence, four thermocouples were placed at  $x = 0.0, -0.5, -1.0$  and  $-1.8$  cm in the center of the specimen and four thermocouples at  $x = 0.0, 0.5, 1.0$  and  $1.8$  cm along the inside wall of the sample holder. In order to suppress the heat transport through the loading arm, a plastic disk was placed on the top of an aluminum disk. The diameter of these two disks was slightly less than the inner diameter of the test cell so that the disks smoothly slid upward during the test.

In Figure 3a only one soil specimen is shown. However, in all freezing tests two duplicated soil specimens were tested simultaneously under the same condition to confirm the reproducibility of



a. Schematic of test apparatus.

1. Soil specimen.
2. Load.
3. Loading arm.
4. Dial gauge.
5. Offset bar.
6. Upper load-guide bar.
7. Lower load-guide bar.
8. Water reservoir.
9. Counterweight.



b. Test apparatus.

c. Schematic of test cell.

- |                    |   |
|--------------------|---|
| 1. Plastic disk.   | 11. Glass beads.  |
| 2. Upper cylinder. | 12. Lower cylinder.   |
| 3. Aluminum disk.  | 13. Cold bath.  |
| 4. Frozen soil.    | 14. Position of the top surface of a soil specimen before freezing. |
| 5. Teflon tape.    | 15. Freezing front.   |
| 6. Thermocouple.   | 16. Initial water head.   |
| 7. Sample holder.  | 17. Thermal insulator.  |
| 8. Unfrozen soil.  | 18. Warm bath.  |
| 9. Loading arm.    | 19. Direction of water flow.  |
| 10. O-ring.        |   |

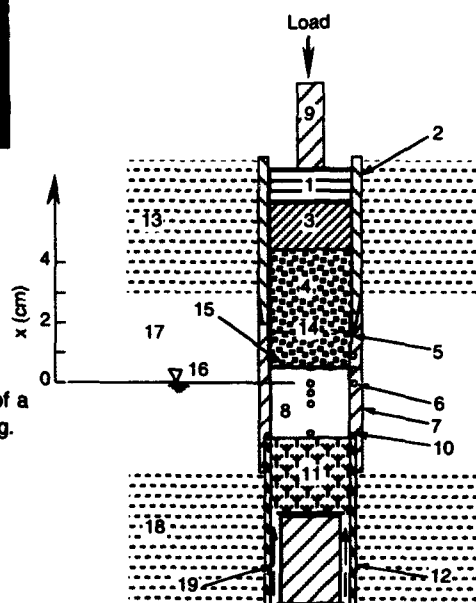


Figure 3. Test apparatus and test cell.

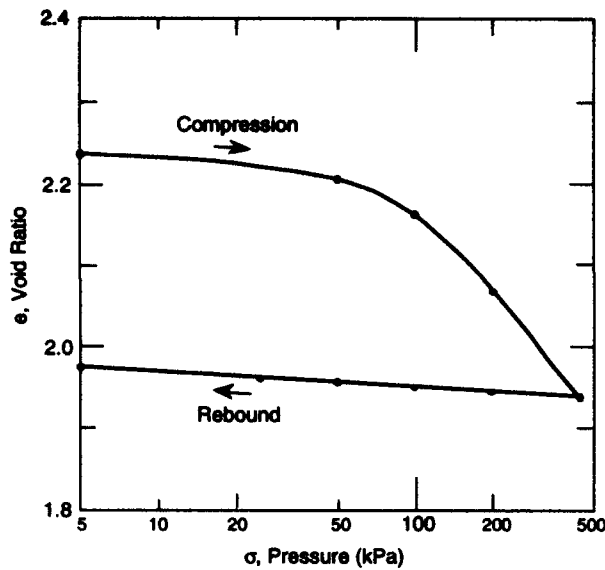


Figure 4. Consolidation characteristics ( $e$  vs.  $\sigma$  kPa) of Kanto loam.

test results. Kanto loam was used as a soil specimen. The properties of this soil were described in the previous paper (Takeda and Nakano 1990). A sample soil was mixed with water to make a de-aired slurry. The slurry was placed in a sample holder and was consolidated in steps to a final pressure 400 kPa in 10 days. Then the consolidated specimen was kept under a given test pressure  $\sigma$  ( $\leq 390$  kPa) for more than 48 hours to become equilibrated.

The data on the relationship between the void ratio  $e$  and the applied pressure  $\sigma$  in the rebound process are presented in Figure 4. From the data we find that the variation of  $e$  in the whole range of  $\sigma < 400$  kPa amounts to 2% at most. Although the variation of  $e$  itself is negligibly small, some of physical properties such as the hydraulic conductivity may be affected significantly by such a small variation. We will further discuss the effects of  $e$  in the following report.

The temperature  $T_c$  of the cold bath and the temperature  $T_w$  of the warm bath were kept constant at specified values for more than 12 hours so that the temperature profile in the specimen would reach a thermal equilibrium. The specified values of  $T_c$  were between  $0^\circ\text{C}$  and  $-2^\circ\text{C}$ . The freezing test began with the ice nucleation induced by putting a very small piece of ice on the top surface of the specimen.

At the beginning of the test the freezing front  $n_1$  rapidly penetrated into the specimen. By changing the temperatures  $T_c$  and/or  $T_w$  in steps, we could stop the freezing front  $n_1$  in a specified region,  $0 < x < 1.0$  cm. We let an ice layer grow in the specified region for two reasons. First, one of four thermocouples for measuring temperatures in the unfrozen part of the specimen was located at  $x = 0.0$  cm. Secondly, the hydraulic condition in our tests was specified by the distance  $\delta_0$  between  $n_0$  and  $n$ , where  $n$  is defined as the interface between the glass beads and the specimen and the pressure of water was kept at the atmospheric pressure. Therefore, it was important to conduct all tests under nearly the same hydraulic conditions. Since  $n_1$  was intentionally positioned in the region specified above, the measurements of temperature in  $R_2$  were made by the thermocouples along the inside wall of the sample holder. Although the differences between the measured temperature at the center of the specimen and that along the inside wall at  $x = 0.0$  cm were found to be quite small, the temperature measurements in  $R_0$  were more accurate than those in  $R_2$  because the temperature at the center was closer to the average temperature over the cross section of the specimen.

As soon as the freezing front stopped and the thermal field in the specimen attained a steady condition, an ice layer emerged (initiation of ice segregation). From the measured temperature profile we calculated a pair of variables  $(\alpha_i^*, \alpha_u^*)$  where the asterisks denote the values of a pair  $(\alpha_i, \alpha_u)$  at the initiation of ice segregation. As we will show below, the measured temperature profiles in  $R_0$  (or  $R_2$ ) were nearly linear when the steady growth of an ice layer took place. The value of  $\alpha_u$  (or  $\alpha_i$ ) was calculated for the most part from the measured temperatures at the two points nearest to  $n_0$  (or  $n_1$ ) in  $R_0$  (or  $R_2$ ).

As discussed in Nakano and Takeda (1991), the amount of heat transported by convection is much less than that transported by conduction in our experiments and, as the result, the temperature profiles in  $R_0$  (or  $R_2$ ) become nearly linear. After obtaining the first pair, we changed  $T_c$  and/or  $T_w$  such that the freezing front moved a little and a new ice layer emerged at a new site slightly below the previous site. Repeating the same procedure, we obtained

several pairs of  $(\alpha_f^*, \alpha_u^*)$  in the specified region described above. A series of tests were conducted under various applied pressures. The test conditions of all tests are summarized in Table 1.

**Table 1. Test conditions.**

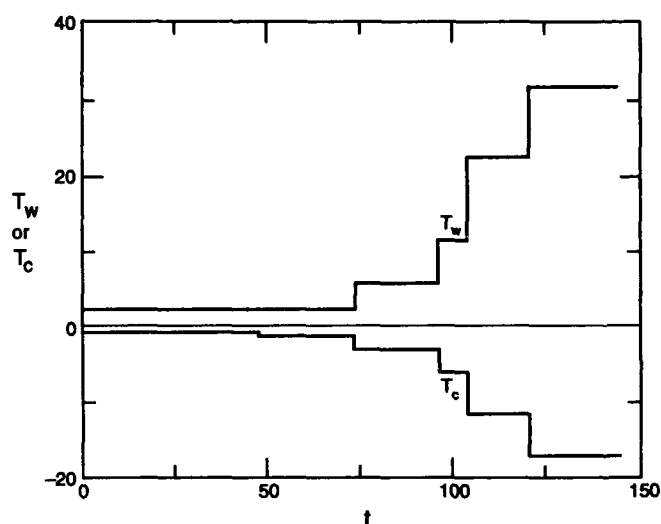
$\sigma$ (kPa)	No. of runs	$T_c$ (°C)	$T_w$ (°C)	No. of pairs ( $\alpha_f^*, \alpha_u^*$ )
0.0	14	-6.1 to -20.0	5.3 to 19.6	14
8.1	4	-3.3 to -14.9	3.0 to 15.1	5
16.2	3	-1.6 to -14.3	1.6 to 14.0	8
48.7	3	-1.3 to -13.5	1.6 to 13.0	6
97.5	2	-1.4 to -16.2	3.0 to 28.2	9
195	2	-1.3 to -17.1	2.0 to 32.2	9
390	2	-2.8 to -18.6	5.0 to 35.8	6

## TEST RESULTS

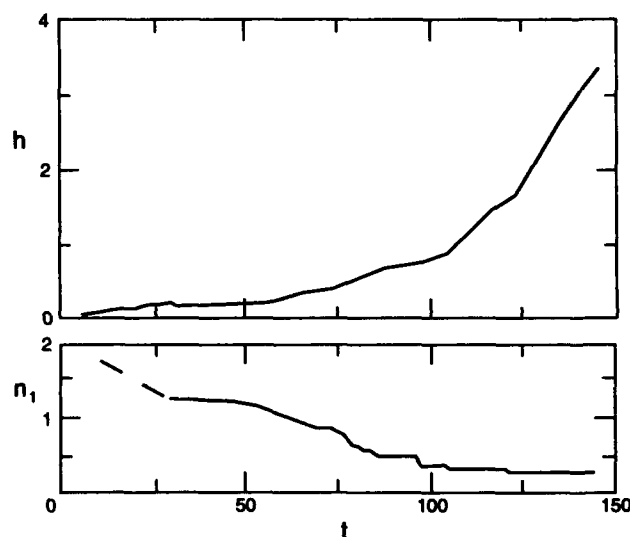
Several variables were measured during the test. The temperature at the location of each thermocouple was measured at least twice every hour, while the amount of heave  $h$  and the location of the freezing front  $n_1$  were measured at least once every hour. The amount of water taken away from the reservoir was measured at suitable intervals, depending upon the amount. The accuracy of these measurements was described in the previous study (Takeda and Nakano 1990).

We will show the behavior of measured variables with time by using the set of data obtained under the applied pressure of 195 kPa as an example. The records of  $T_c$  and  $T_w$  are shown in Figure 5a. Since  $T_c$  and  $T_w$  were changed stepwise, the records look like a step function. Despite the stepwise change of  $T_c$  and  $T_w$ , all other measured variables described above changed more or less continuously with respect to time. The amount of heave  $h$  and the position of  $n_1$  are plotted vs. time in Figure 5b.

The rate of heave  $r$  was calculated from the measured  $h(t)$  as the average over a finite time interval, while the rate of water intake  $f_{10}$  was calculated from the measured amount of water in the reservoir as the average over another finite time interval. The calculated values of  $r$  and  $f_{10}$  are plotted vs. time in Figure 5c where each horizontal line is the average over the time interval corre-

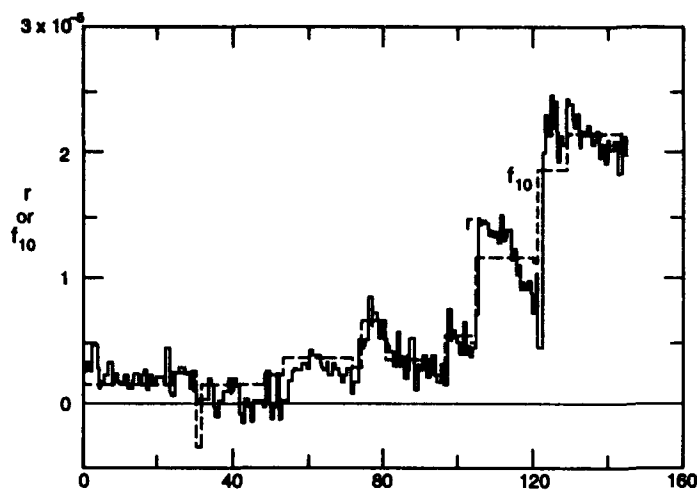


a. Temperatures  $T_c$  °C and  $T_w$  °C vs.  $t$  hours with  $\sigma = 195$  kPa.

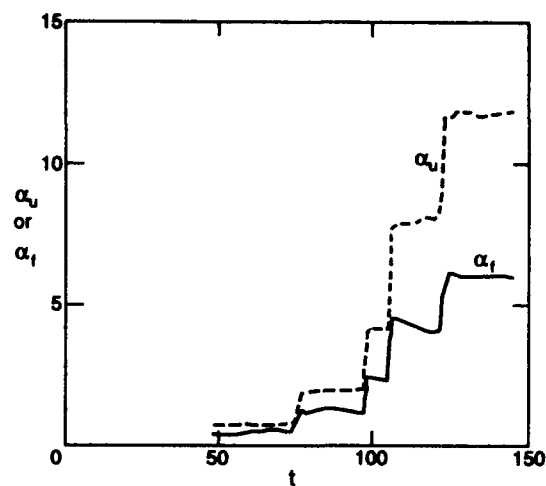


b. Measured  $h$  cm and  $n_1$  cm vs.  $t$  hours with  $\sigma = 195$  kPa.

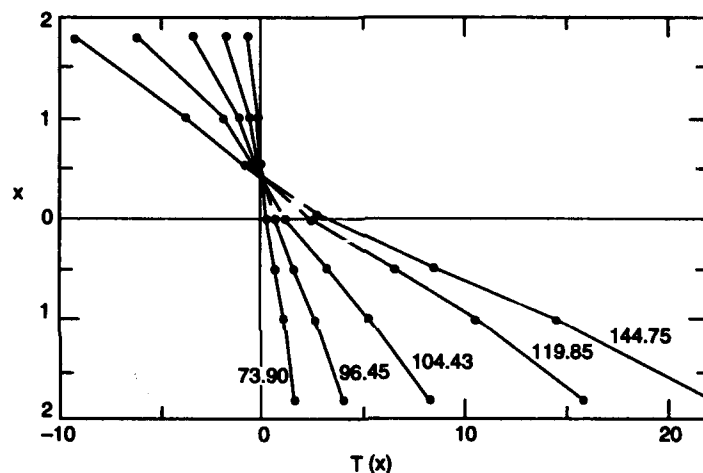
Figure 5. Measured variables vs. time for  $\sigma = 195$  kPa.



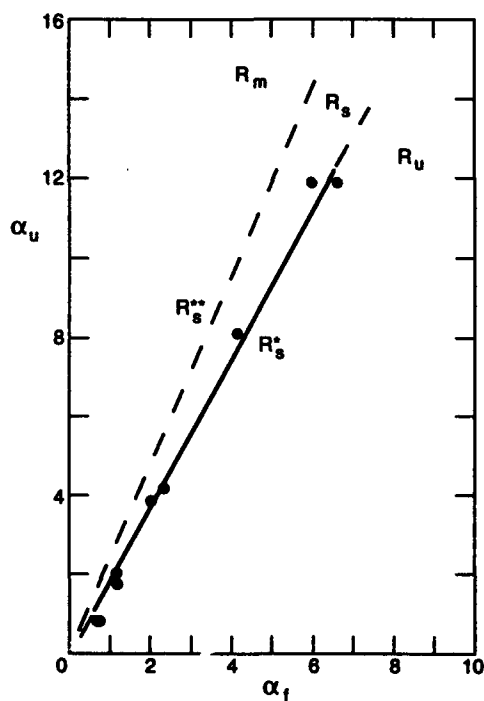
c. Calculated values ( $\text{cm s}^{-1}$ ) of  $r$  and  $f_{10}$  vs.  $t$  hours ( $\sigma = 195$  kPa).



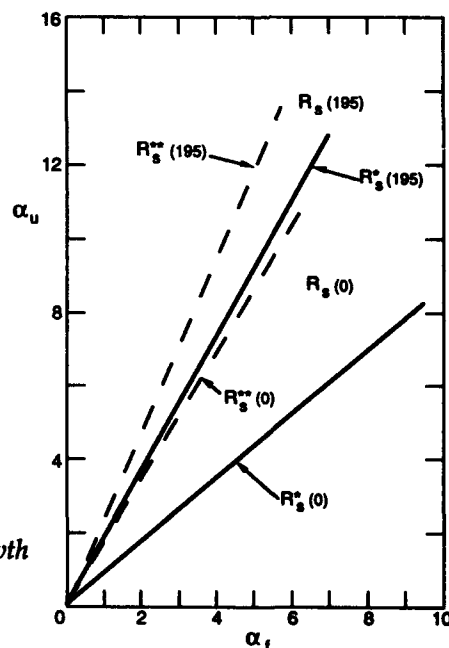
d. Calculated values ( $^{\circ}\text{C cm}^{-1}$ ) of  $\alpha_f$  and  $\alpha_u$  vs.  $t$  hours ( $\sigma = 195$  kPa).



e. Measured temperature profiles  $T(x)^{\circ}\text{C}$  in the specimen at  $t = 73.90, 96.45, 104.43, 119.85$  and  $144.75$  hours ( $\sigma = 195$  kPa).



f. Steady growth region  $R_s$  ( $\sigma = 195$  kPa).



g. Steady growth region  $R_s(\sigma)$ .

Figure 5 (cont'd).

sponding to the line length. Similarly, the calculated average values of  $\alpha_f$  and  $\alpha_u$  from the measured temperature profiles over certain variable intervals are plotted vs.  $t$  in Figure 5d.

The measured temperature profiles in the specimen at 73.90, 96.45, 104.43, 119.85 and 144.75 hours are presented in Figure 5e, where dark circles are data points and straight lines are drawn between two neighboring points. It is easy to see from Figure 5e that each solid line in the frozen or the unfrozen part of the specimen is nearly linear. This implies that the thermal field was nearly steady at each of those points of time when the initiation of ice segregation occurred and a pair of  $(\alpha_f^*, \alpha_u^*)$  were obtained.

At the beginning of this test,  $T_c$  and  $T_w$  were kept constant at  $-0.9^\circ\text{C}$  and  $2.0^\circ\text{C}$ , respectively. The freezing front  $n_1$  moved downward rapidly. At 48.3 hours  $T_c$  was decreased to  $-1.3^\circ\text{C}$  so that the penetrating speed of  $n_1$  would be slowed while  $T_w$  was kept constant. At about 55.0 hours the speed of  $n_1$  increased again and the rate of heave  $r$  began increasing to attain a maximum at 61.0 hours. After 61.0 hours  $r$  decreased and  $n_1$  gradually approached  $x = 0.85$  cm. At 71.4 hours a segregated ice layer without any visible soil particles emerged as soon as  $n_1$  ceased to move. At this time  $r$  became nearly constant and the values of  $\alpha_f$  and  $\alpha_u$  remained constant. Under such a steady condition, the ice layer kept growing while  $n_1$  remained still until 73.9 hours. We found these constant values of  $\alpha_f$  and  $\alpha_u$  to be  $\alpha_f^*$  and  $\alpha_u^*$ , respectively. In other words, a constant pair  $(\alpha_f^*, \alpha_u^*)$  was on  $R_s^*$ .

After obtaining the first pair  $(\alpha_f^*, \alpha_u^*)$ , we changed  $T_c$  and  $T_w$  in such a manner that  $n_1$  moved downward slightly and a new ice layer emerged at a new location slightly below the previous ice layer. Repeating the same procedure, we obtained several pairs of  $(\alpha_f^*, \alpha_u^*)$ . As shown in Figure 5d, it took a few hours for  $\alpha_f$  and  $\alpha_u$  to stabilize after  $T_c$  and/or  $T_w$  were changed stepwise. It is clear from Figures 5c and 5d that the values of  $r$  and  $f_{10}$  were sensitively affected by minor variations of  $\alpha_f$  and  $\alpha_u$ . When  $r$  is quite small, accurate measurement of the rate of water intake over a short time interval was difficult. Therefore, the mass flux of water was usually calculated based on  $r$  under such a case.

From two tests under the condition of  $\sigma = 195$  kPa, we obtained nine pairs of  $(\alpha_f^*, \alpha_u^*)$  that are plotted in the diagram of temperature gradients in Figure 5f. As in the previous study (Takeda and Nakano 1990), we will seek a linear approximation to the relation between  $\alpha_f^*$  and  $\alpha_u^*$  given as:

$$\alpha_u^* = S(\sigma) \alpha_f^* \quad (10)$$

where the positive proportionality factor  $S$  is assumed to depend on only the applied pressure  $\sigma$ . Using the method of interval estimate (Fisz 1965), we have found from the data set that the value of  $S(195)$  is 1.856. The line  $R_s^*(195)$  passing through the data points in Figure 5f is given by eq 10 with  $\sigma = 195$  kPa, which is a linear approximation to the boundary  $R_s^*$  that divides the steady growth region  $R_s$  and the region  $R_u$  where the steady growth of an ice layer does not occur.

The broken line  $R_s^{*+}(195)$  in Figure 5f is given as:

$$\alpha_u = [k_1(\sigma)/k_0] \alpha_f, \quad \sigma = 195 \text{ kPa.} \quad (11)$$

We found empirically that the thermal conductivity  $k_0$  of the unfrozen part of a specimen is hardly affected by the applied pressure  $\sigma$ . However,  $\sigma$  affects the thermal conductivity  $k_1$  of an ice layer to a degree that is minor but not negligible. The measured average densities  $d_2$  and conductivities  $k_1$  of ice layers under various  $\sigma$  values are presented in Table 2. It is easy to see that the values of  $d_2$  when  $\sigma > 0$  are greater than when  $\sigma = 0$ . The applied pressure evidently reduces the amount of space occupied by air in ice layers and, as a result, the values of  $k_1$  when  $\sigma > 0$  are also greater than when  $\sigma = 0$  as shown in Table 2.

Table 2. Summary of test results.

$\sigma$ (kPa)	$S(\sigma)$	$d_2$ (g cm <sup>-3</sup> )	$k_1$ J (cm s °C) <sup>-1</sup>	$k_1 k_0^{-1}$ *
0.0	0.871	0.860	1.59E-2†	1.73
8.1	1.078	0.898	2.13E-2	2.31
16.2	1.554	0.895	2.12E-2	2.30
48.7	1.618	0.907	2.19E-2	2.38
97.5	1.817	0.906	2.18E-2	2.37
195	1.856	0.907	2.19E-2	2.38
390	1.985	0.904	2.17E-2	2.36

\*  $k_0 = 9.20 \times 10^{-3}$  J/(cm s °C).

†  $E - N = 10^{-N}$ .

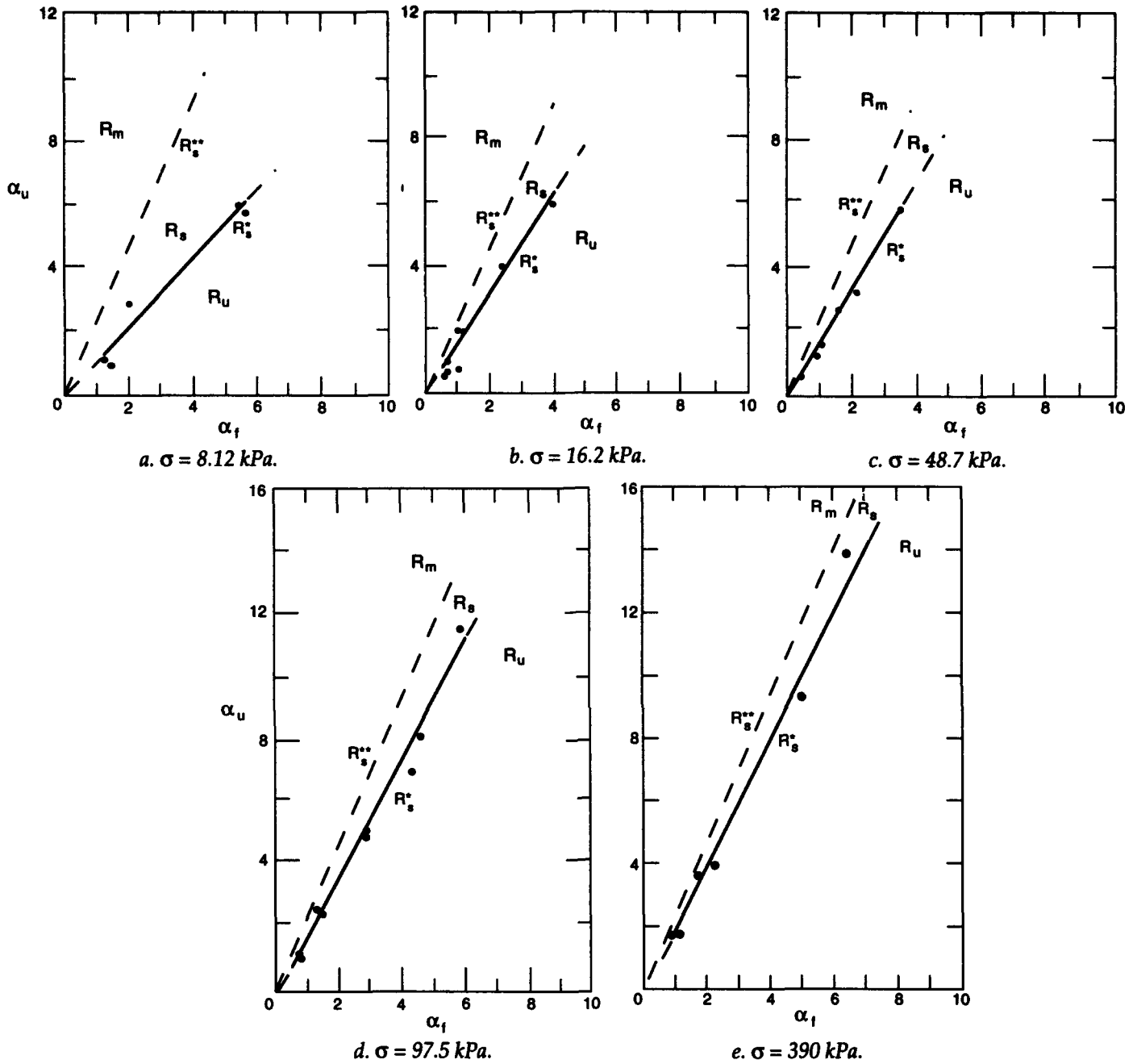


Figure 6. Steady growth region  $R_s$ .

The values of  $(k_1/k_0)$  with  $\sigma = 195$  kPa and  $\sigma = 0.0$  kPa are 2.38 and 1.73, respectively, as given in Table 2. Because of this difference the broken line  $R_s^{**}(0)$  given by eq 11 with  $\sigma = 0.0$  lies below the line  $R_s^{**}(195)$  as shown in Figure 5g. The steady growth region  $R_s(195)$  under  $\sigma = 195$  kPa is the region bounded by  $R_s^*(195)$  and  $R_s^{**}(195)$  while that under  $\sigma = 0.0$  kPa is the region bounded by  $R_s^*(0)$  and  $R_s^{**}(0)$  in Figure 5g. It is clear from this figure that the applied pressure of 195 kPa significantly reduced the area of the steady growth region.

Using the same test procedure as described above for the case of  $\sigma = 195$  kPa, we conducted a series of tests under various applied pressures to determine the region of steady growth  $R_s(\sigma)$  for a given  $\sigma$ . The results of these tests are presented in Figure 6a ( $\sigma = 8.12$  kPa), 6b (16.2 kPa), 6c (48.7 kPa), 6d (97.5 kPa) and 6e (390 kPa). It is clear from Figures 5g and 6 that the region of steady growth  $R_s(\sigma)$



tends to decrease with increasing  $\sigma$ . The values of  $S(\sigma)$  given in Table 2 are plotted vs.  $\sigma$  in Figure 7. It is found from Figure 7 that the value of  $S$  increases sharply with increasing  $\sigma$  when  $\sigma$  is small and that the rate of increase slows down as  $\sigma$  becomes greater. A curve in Figure 7 is one example of the approximate presentation of data points given as

$$S(\sigma) = 0.280 \sigma^{0.243} + 0.856 \quad (12)$$

where  $\sigma$  is in kilopascals.

We have found empirically (Takeda and Nakano 1990) that there is the upper bound  $A_1$  (or  $A_0$ ) of  $\alpha_f$  (or  $\alpha_u$ ) beyond which an ice layer with cavities grows when  $\sigma$  is negligibly small and that the value of  $A_1$  for Kanto loam is  $8.8^\circ\text{C cm}^{-1}$ . The reason for such behavior was explained (Takeda and Nakano 1990, Nakano and Takeda 1991) as follows. The pressure  $P_{10}$  of water at  $n_0$  decreases with the increasing value of  $\alpha_f$  (or  $f_{10}$ ) until  $P_{10}$  attains a value that corresponds to the air entry value of Kanto loam when an ice layer with cavities begins growing. The growth of an ice layer with cavities was not observed in all the tests under various applied pressures presented in this work. Consequently, we were unable to confirm the upper bound of  $\alpha_f$  in this work.

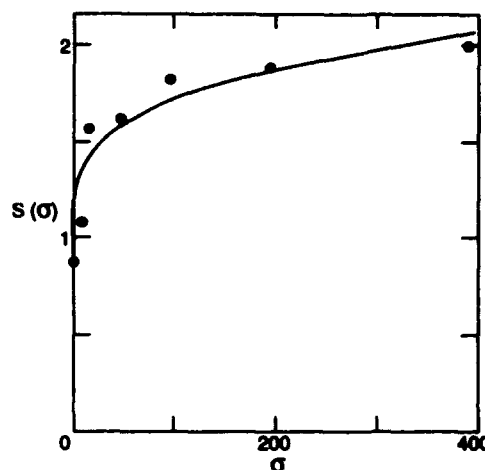


Figure 7. Values of  $S(\sigma)$  vs.  $\sigma$  (kPa).

## CONCLUSIONS

A series of freezing tests on Kanto loam were conducted under various overburden pressures to find the steady growth condition of a segregated ice layer. The steady growth condition was found to be determined by the absolute value of the temperature gradient of the unfrozen part of the soil  $\alpha_u$  near the  $0^\circ\text{C}$  isotherm and that of the frozen part of the soil  $\alpha_f$  near the warmest end of an ice layer under given hydraulic condition and applied effective pressure as follows:

$$\alpha_u = A\alpha_f, \quad k_1/k_0 > A > S(\sigma) \quad (13)$$

where  $S(\sigma)$  is an increasing function of  $\sigma$ .

This is the first of a two-part presentation on the effects of applied pressure on the steady growth condition of an ice layer. In the following paper we will show that the model  $M_1$  is consistent with experimental data presented in this work.

## LITERATURE CITED

- Beskow, G. (1935) Soil freezing and frost heaving with special attention to roads and railroads. *Swedish Geological Society Yearbook*, Series C, 26(3): 1-145.
- Edlefsen, N.W. and A.B.C. Anderson (1943) Thermodynamics of soil moisture. *Hilgardia*, 15(2): 31-298.
- Fisz, M. (1965) *Probability Theory and Mathematical Statistics*. New York: John Wiley & Sons, p. 461.
- Ishizaki, T. and N. Nishio (1985) Experimental study of final ice lens growth in partially frozen saturated soil. In *Proceedings, 4th International Symposium on Ground Freezing, 5-7 August, Sapporo, Japan* (S. Kinoshita and M. Fukuda, Ed.). Rotterdam, Netherlands: A.A. Balkema, p. 71-78.
- Konrad, J.M. and N.R. Morgenstern (1980) A mechanistic theory of ice lens formation in fine-grained soils. *Canadian Geotechnical Journal*, 17: 473-486.

- Konrad, J.M. and N.R. Morgenstern (1981) The segregation potential of a freezing soil. *Canadian Geotechnical Journal*, 18: 482-491.
- Konrad, J.M. and N.R. Morgenstern (1982) Effects of applied pressure on freezing soils. *Canadian Geotechnical Journal*, 19: 494-505.
- Nakano, Y. (1990) Quasi-steady problems in freezing soils: I. Analysis on the steady growth of an ice layer. *Cold Regions Science and Technology*, 17(3): 207-226.
- Nakano, Y. and K. Takeda (1991) Quasi-steady problems in freezing soils: III. Analysis on experimental data. *Cold Regions Science and Technology*, 19: 225-243.
- Radd, F.J. and D.H. Oertle (1973) Experimental pressure studies of frost heave mechanism and the growth-fusion behavior of ice. In *Permafrost: The North American Contribution to the 2nd International Conference on Permafrost, Yakutsk, 13-28 July*. Washington, D.C.: National Academy of Sciences, p. 377-384.
- Taber, S. (1929) Frost heaving. *Journal of Geology*, 37(1): 428-461.
- Taber, S. (1930) The mechanics of frost heaving. *Journal of Geology*, 38: 303-317.
- Takashi, T., T. Ohrai, H. Yamamoto and J. Okamoto (1981) Upper limit of heaving pressure derived by pore-water pressure measurements of partially frozen soil. *Engineering Geology*, 18: 245-257.
- Takeda, K. and Y. Nakano (1990) Quasi-steady problems in freezing soils: II. Experiment on steady growth of an ice layer. *Cold Regions Science and Technology*, 18: 225-247.

# REPORT DOCUMENTATION PAGE

Form Approved  
OMB No. 0704-0188

Public reporting burden for this collection of information is estimated to average 1 hour per response, including the time for reviewing instructions, searching existing data sources, gathering and maintaining the data needed, and completing and reviewing the collection of information. Send comments regarding this burden estimate or any other aspect of this collection of information, including suggestion for reducing this burden, to Washington Headquarters Services, Directorate for Information Operations and Reports, 1215 Jefferson Davis Highway, Suite 1204, Arlington, VA 22202-4302, and to the Office of Management and Budget, Paperwork Reduction Project (0704-0188), Washington, DC 20503.

1. AGENCY USE ONLY (Leave blank)		2. REPORT DATE November 1993		3. REPORT TYPE AND DATES COVERED	
4. TITLE AND SUBTITLE  Growth Condition of an Ice Layer in Freezing Soils Under Applied Loads: I. Experiment				5. FUNDING NUMBERS  PE: 6.11.02A PR: 4A161102AT24 TA: SC WU: F01	
6. AUTHORS  Kazuo Takeda and Yoshisuke Nakano					
7. PERFORMING ORGANIZATION NAME(S) AND ADDRESS(ES)  Konoike Construction Co., Ltd. and U.S. Army Cold Regions Research Konohana, Osaka, Japan and Engineering Laboratory 72 Lyme Road Hanover, New Hampshire 03755-1290				8. PERFORMING ORGANIZATION REPORT NUMBER  CRREL Report 93-21	
9. SPONSORING/MONITORING AGENCY NAME(S) AND ADDRESS(ES)  Office of the Chief of Engineers Washington, D.C. 20314-1000				10. SPONSORING/MONITORING AGENCY REPORT NUMBER	
11. SUPPLEMENTARY NOTES					
12a. DISTRIBUTION/AVAILABILITY STATEMENT  Approved for public release; distribution is unlimited.  Available from NTIS, Springfield, Virginia 22161.				12b. DISTRIBUTION CODE	
13. ABSTRACT (Maximum 200 words)  A series of freezing tests on Kanto loam were conducted under various overburden pressures to find the steady growth condition of a segregated ice layer. The steady growth condition was found to be determined by the absolute value of the temperature gradient of the unfrozen part of the soil $\alpha_u$ near the 0°C isotherm and that of the frozen part of the soil $\alpha_f$ near the warmest end of an ice layer under given hydraulic conditions and applied effective pressure $\sigma$ as follows: $\alpha_u = A\alpha_f$ , $k_1/k_0 > A > S(\sigma)$ ; where $k_1$ and $k_0$ are the thermal conductivities of the frozen and unfrozen parts, respectively, $A$ is a constant and $S$ is an increasing function of $\sigma$ . This is the first of a two-part presentation on the subject; the analytical aspects of the study are presented in a second report.					
14. SUBJECT TERMS  Freezing fronts Freshwater ice  Frozen soils Ice lenses  Mathematical analysis				15. NUMBER OF PAGES 19	
				16. PRICE CODE	
17. SECURITY CLASSIFICATION OF REPORT  UNCLASSIFIED	18. SECURITY CLASSIFICATION OF THIS PAGE  UNCLASSIFIED	19. SECURITY CLASSIFICATION OF ABSTRACT  UNCLASSIFIED	20. LIMITATION OF ABSTRACT  UL		